HIFiRE-1 Turbulent Shock Boundary Layer Interaction – Flight Data and Computations

Roger L. Kimmel*
Air Force Research Laboratory, 2130 8th St., WPAFB, OH 45433, USA

Dinesh Prabhu†
NASA Ames Research Center, Moffett Field, California 94035

The Hypersonic International Flight Research Experimentation (HIFiRE) program is a hypersonic flight test program executed by the Air Force Research Laboratory (AFRL) and Australian Defence Science and Technology Organisation (DSTO). This flight contained a cylinder-flare induced shock boundary layer interaction (SBLI). Computations of the interaction were conducted for a number of times during the ascent. The DPLR code used for predictions was calibrated against ground test data prior to exercising the code at flight conditions. Generally, the computations predicted the upstream influence and interaction pressures very well. Plateau pressures on the cylinder were predicted well at all conditions. Although the experimental heat transfer showed a large amount of scatter, especially at low heating levels, the measured heat transfer agreed well with computations. The primary discrepancy between the experiment and computation occurred in the pressures measured on the flare during second stage burn. Measured pressures exhibited large overshoots late in the second stage burn, the mechanism of which is unknown. The good agreement between flight measurements and CFD helps validate the philosophy of calibrating CFD against ground test, prior to exercising it at flight conditions.

I. Introduction

The Hypersonic International Flight Research Experimentation (HIFiRE) program consists of extensive ground tests and computation focused on specific hypersonic flight technologies.[1,2] Its purpose is to develop and validate technologies critical to next generation hypersonic aerospace systems. Candidate technology areas include, but are not limited to, propulsion, propulsion-airframe integration, aerodynamics and aerothermodynamics, high temperature materials and structures, thermal management strategies, guidance, navigation, and control, sensors, and system components. Each technology program is designed to culminate in a flight test. The first science flight of the HIFiRE series, HIFiRE-1, launched 22 March 2010 at the Woomera Prohibited Area in South Australia at 0045 Universal Coordinated Time (UTC) (1045 local time).

The primary objective of HIFiRE-1 was to measure aerothermal phenomena in hypersonic flight. The primary experiment consisted of boundary-layer transition measurements on a 7-deg half angle cone with a 2.5 mm radius nose. The secondary aerothermal experiment was a shock-boundary-layer interaction created by a 33-deg-flare / cylinder configuration. HIFiRE-1 ground test and computation created an extensive knowledge base regarding transition and shock boundary-layer interaction (SBLI) on axisymmetric bodies. This research has been summarized in numerous prior publications.[3,4,5,6,7,8,9,10,11,12,13,14]

Preliminary results from the HIFiRE-1 aerothermal experiments have been previously published.[15] Ref. 15 presented preliminary results from both the BLT and SBLI experiments during ascent and descent. Although the vehicle was at a higher angle of attack than intended during descent, the payload instrumentation scheme permitted acquisition of interesting and useful high angle-of-attack (AoA) transition data. [16,17] Analysis of the high AoA reentry SBLI experiment is considerably more difficult, so the current paper focuses only on the ascent-phase SBLI. A prior publication expanded on the SBLI experiment focused on unsteady pressure measurements.[18] The current publication focuses on comparing computations of the SBLI to flight measurements for the ascent phase of flight.

---

* Principal Aerospace Engineer, Associate Fellow AIAA.

† Senior Research Scientist, Entry Systems and Technology Division; currently ERC, Inc., Mail Stop 229-1. Associate Fellow AIAA.

HIFiRE-1 presents an unusual test case for CFD, since highly-detailed surface measurements were made on a relatively simple configuration. Although the flight conditions were relatively benign, with a maximum Mach number of seven during reentry, computation of the turbulent SBLI is not trivial. Although CFD codes can be calibrated against wind tunnel results prior to applying them to flight conditions, it is generally not possible to match flight conditions exactly in ground test. HIFiRE-1 showed significant variations in flight conditions and wall temperatures during ascent. Freestream unit Reynolds numbers ranged from 0 to 60×10^6 per meter during ascent, and ascent Mach number varied from subsonic to approximately 5.5. Flare temperatures ranged from approximately 300 K to a peak of 540 K during ascent, and at any time varied significantly over the length of the vehicle. Computation of the HIFiRE-1 ascent turbulent SBLI provides a strong test of a computer code calibrated against a point condition in a wind tunnel.

II. Experiment and Flight Profile

The HIFiRE-1 vehicle has been described in several prior publications, most notably in Ref. 14. The overall payload dimensions and the different payload modules are shown in Fig. 1. The experiments were carried out on the forward sections of the payload including a cone, a cylinder, and a flare that transitioned to the diameter of the second stage motor (0.356 m). The nose tip consisted of an iridium-coated, titanium-zirconium-molybdenum (TZM) alloy. The surface finish of the nose tip after coating was measured to be 6-8 microinches (0.15-0.2 microns) RMS (root mean square). The aluminum cone shell was finished to a 0.8 micron R_a finish (R_a is the arithmetic average of roughnesses). The cone half angle of seven degrees was chosen to match configurations used in preceding ground tests and analytical/numerical work. The aft-portion of the cylinder and the flare consisted of AISI 1045 steel.

The payload contained duplicate instrumentation on rays 180^o apart, permitting a cross-check between instrumentation on these two rays. One ray of instrumentation contained a diamond-shaped trip to produce a roughness-induced transition. The payload incorporated this feature to ensure that turbulent data might be obtained even if the reentry portion of the flight terminated before natural transition occurred. Pressures and temperatures on the flare on this ray were recorded throughout flight. The circuit board that conditioned SBLI pressures on the cylinder on this ray failed at approximately t=6 seconds, therefore no data were recorded from these instruments after this time.

The ray of instrumentation 180^o opposite of the trip contained no intentional trip element. However, backward-facing steps on the nosetip of the vehicle tripped transition for $t<11.5$ seconds. For $t>11.5$ seconds, transition moved aft with time over the conical portion of the vehicle, until about $t=21.5$ seconds. At this point, flow over the cone was entirely laminar. The SBLI began to take on characteristics of a transitional interaction at about this time.

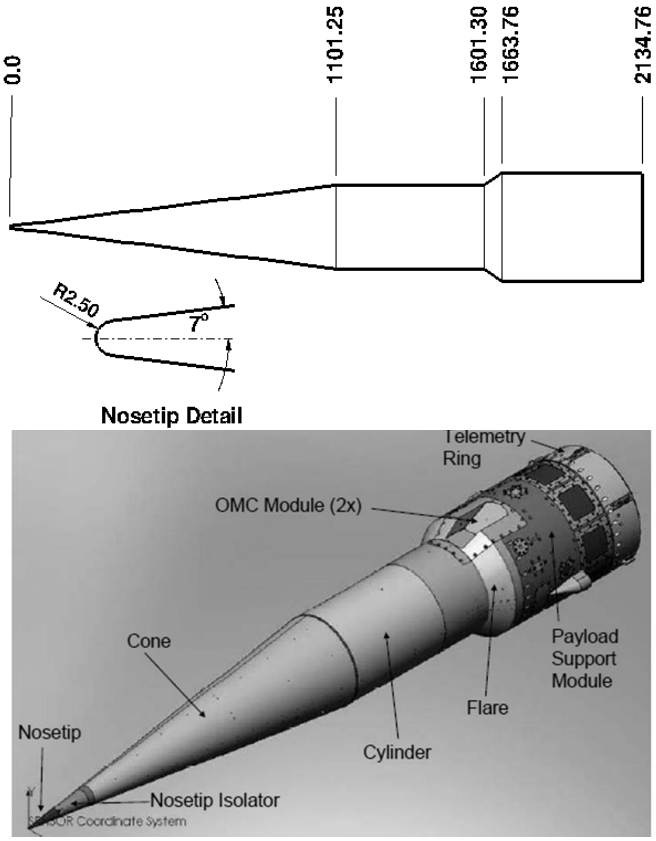

Fig. 1 HIFiRE-1 payload configuration, dimensions in mm

The payload flew a ballistic trajectory similar to those employed for the HyShot[19] and Hypersonic Collaborative Australia/United States Experiment (HyCAUSE)[20] flights. The as-flown trajectory is shown in Fig. 2. The Terrier first stage burnt for 6.3 seconds and was then drag-separated from the second stage. The Orion/payload combination coasted until the second stage ignited at 15 seconds. Orion burnout occurred at 43 seconds. The payload remained attached to the second stage throughout the entire flight to provide stability as the payload reentered the atmosphere. Approximately the first and last 45 seconds of the trajectory were endoatmospheric. The remainder of the trajectory was exoatmospheric.

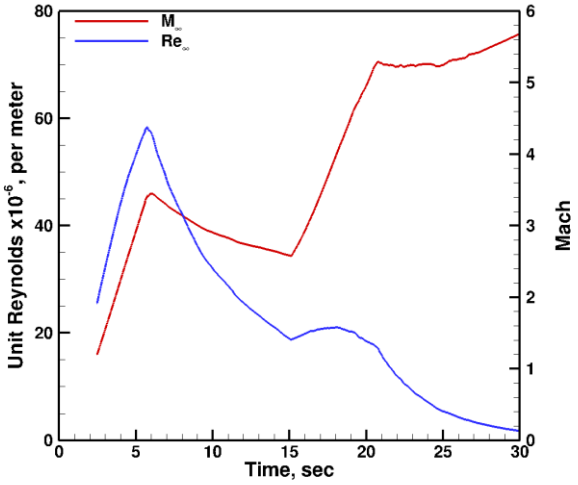

Fig. 2 HIFiRE-1 as-flown trajectory

A prior publication described the HIFiRE-1 mission.[21] The most notable complications in the mission were failures of the on-board Global Positioning System (GPS) and the exoatmospheric pointing maneuver. The loss of the GPS meant that the vehicle altitude and velocity had to be reconstructed from existing data such as accelerometers, radar tracks, etc. References 15 and 21 describe development of the best estimated trajectory (BET). The failure of the exoatmospheric pointing maneuver was a more serious malfunction, since it caused the vehicle to enter the atmosphere with an angle of attack as high as 40-deg. Although angle-of-attack oscillations damped and decreased as the vehicle descended, the payload angle of attack was still over 10-deg as aerothermal data began to be collected during descent. Since the risk of this occurrence was recognized prior to flight, the payload flew unshrouded, i.e. no nosecone shell covered the experiment during ascent. This permitted low-angle-of-attack (< 1 deg) data to be obtained during ascent. This paper will focus on the low AoA ascent data. Since the high AoA during reentry makes interpretation of the SBLI experiment difficult, analysis of this portion of the flight is deferred.

III. Instrumentation

The primary aerothermal instrumentation for HIFiRE-1 consisted of Medtherm Corporation coaxial thermocouples. Type E (chromel-constantan) were installed in the SBLI region. Kulite® pressure transducers measured local static pressures. Figure 3 illustrates the transducer layout. All pressure transducers with the exception of those in the flare were model XCE-093. Those in the flare were XTEH-7LAC-190 (M). The flare transducers each output separate AC and DC-coupled signals that were digitized on different channels.

The coaxial thermocouples were dual-junction models that measured front-surface and back-surface (internal) temperatures simultaneously. These thermocouples were bonded into pre-drilled holes in the model surface using LOCTITE® adhesive. The thermocouples were installed with the backface junction flush to within 0.1 mm (estimated) of the model interior surface. The portion of the thermocouple which extended beyond the model external surface was removed using files and abrasives so that the final thermocouple contour matched the model surface contour. This finishing process created a "sliver junction" between the center-wire and annular thermocouple materials, in which whiskers of one conductor are dragged over the other to create the thermocouple junction.

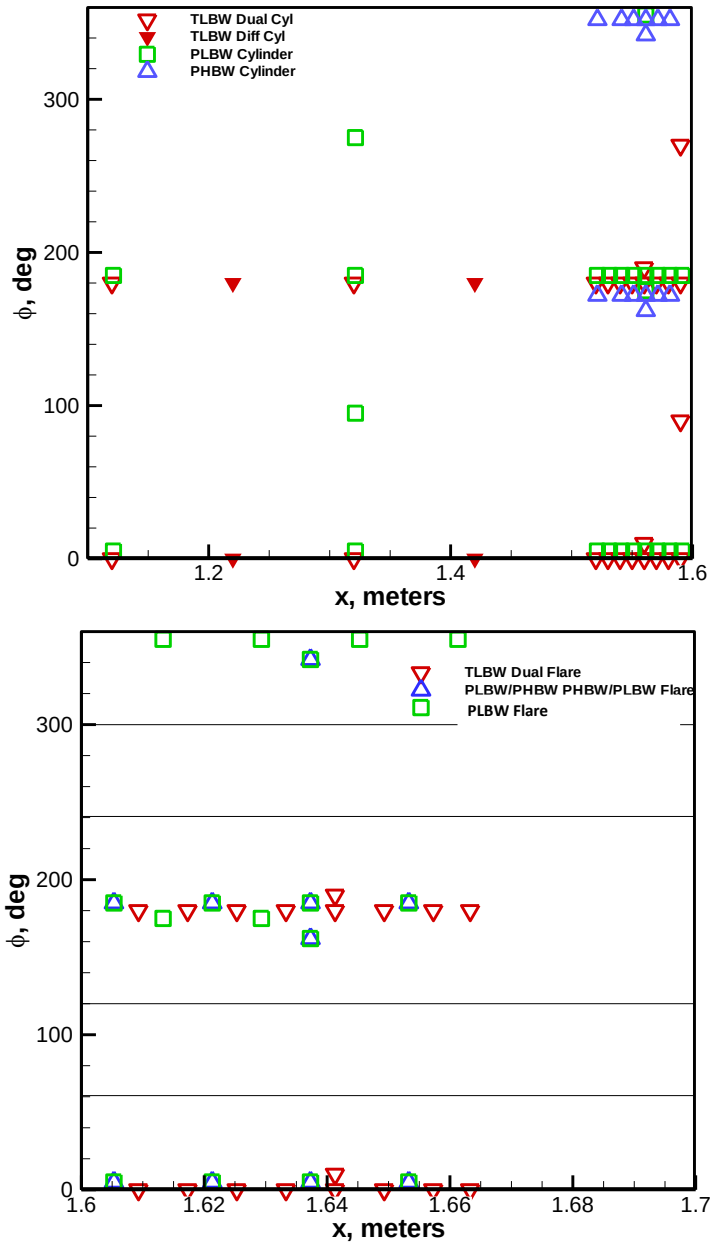

Figure 3 SBLI Transducer Layouts

IV. Computations

The computations proceeded in two stages. The first stage of computations consisted of calculations for test results from the CUBRC LENS wind tunnel. This permitted several transport models to be evaluated at wind tunnel conditions prior to employing them on the flight vehicle. Run 30 with M=7.19 and unit Reynolds Re=9.5x10^6/m, and α=0 was used as a test case. The model was full-scale, with a nose radius of 2.5 mm, identical to the flight configuration. The flare of the model was extended downstream to a larger diameter than the flight vehicle to ensure that attachment and equilibrium occurred on the flare. The focus of this effort was on the SBLI. In these calculations, turbulent transport was based on the SST turbulence model with and without a compressibility correction. Laminar flow assumed a constant Prandtl number Pr=0.7. Wall temperature in the computations was constant at T_w=300K. Transition was forced in the computations to match the wind tunnel transition location. Results shown in Figure 4 indicate that the Menter SST model, without compressibility correction, gave the best

correlation with pressure and heat transfer measured in the SLBI. These results are in agreement with those of Maclean.[12] Also, computations with the SST model where boundary layer transition is near the nosetip, and ones where transition is forced in the computation near where it occurred in the test, show little effect of transition location on the SBLI pressures.

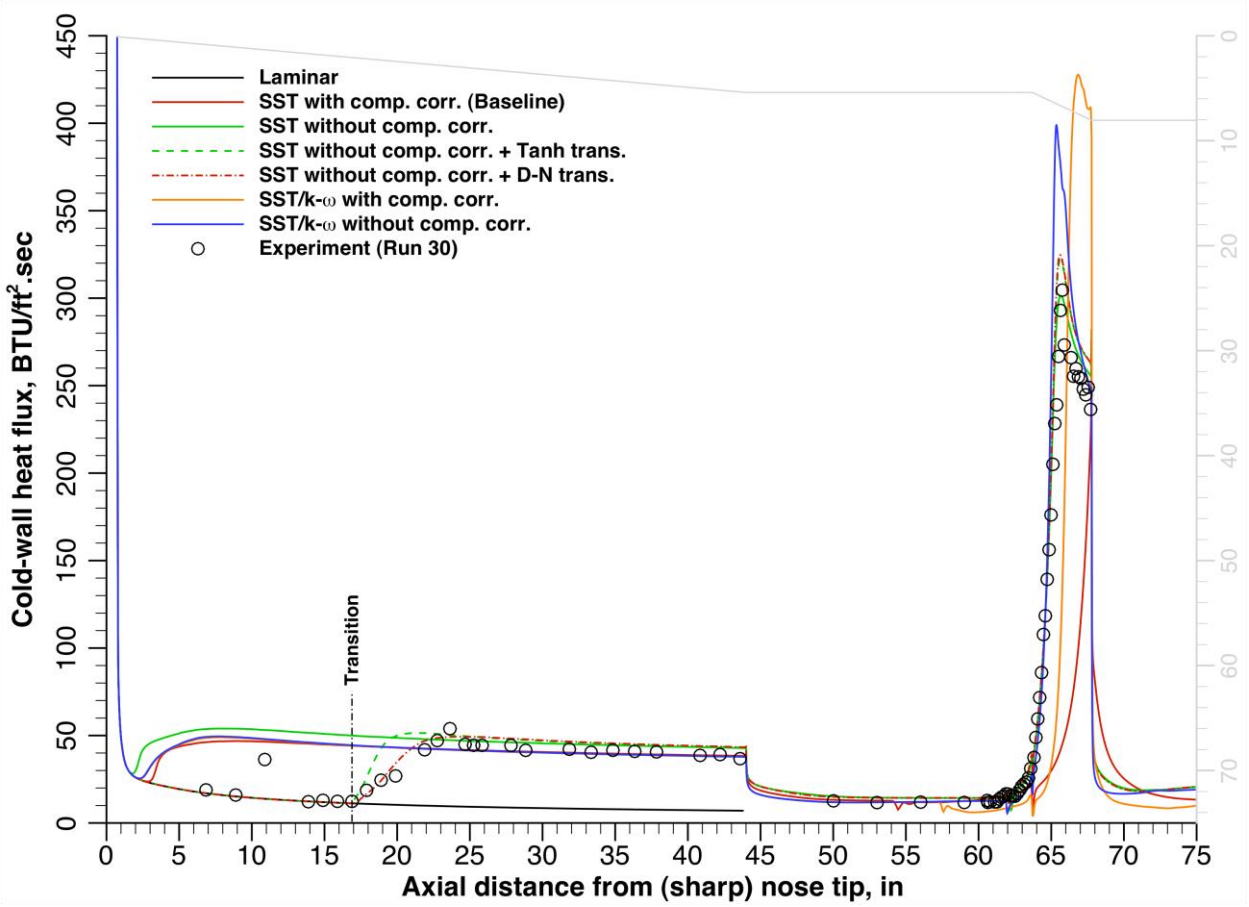

Figure 4 Computation of CUBRC run 30 with varying transport models and boundary conditions

In the second stage of computations, the entire flight vehicle was computed at a number of different times during the ascent. Two grids were used for these analyses. A 1633x537 grid was for $4.5 \leq t \leq 19.5$ s., and a 1632x367 grid was used for $20.5 \leq t \leq 23.5$ s. Calculations were carried out for wall temperatures of T_w= 300, 400 and 500K, approximately bounding the flight vehicle wall temperatures.

The effect of the boundary layer transition location on the SBLI was examined, but seemed to have little effect on computed results where transition was well upstream of the flare. Figure 5 shows measured and computed laminar and turbulent heat transfer on the cone at four times during ascent. For t=5.5 and 6 seconds, the measured heat transfer correlates well with predicted turbulent values. For t=15.5 and 21.5 seconds, the transition from laminar to turbulent heating on the cone is apparent.

Even though the cone contains a region of turbulent flow over its aft portion at t=21.5 seconds, measurements on the smooth-side SBLI begin to deviate from the tripped side slightly before this time. This departure is evident in Figure 6, which shows smooth and rough-side temperatures on the first transducer on the flare downstream of the corner. Temperatures on both sides of the payload agree well until t=20 seconds. At this point, temperatures on the smooth side begin to rise and spike at approximately t=22 seconds. After this, temperatures decay. It is surmised that this behavior is due to the transitional nature of the flow over the smooth side of the payload. Therefore, comparisons between measured and computed SBLI quantities will be constrained to times less than 20 seconds.

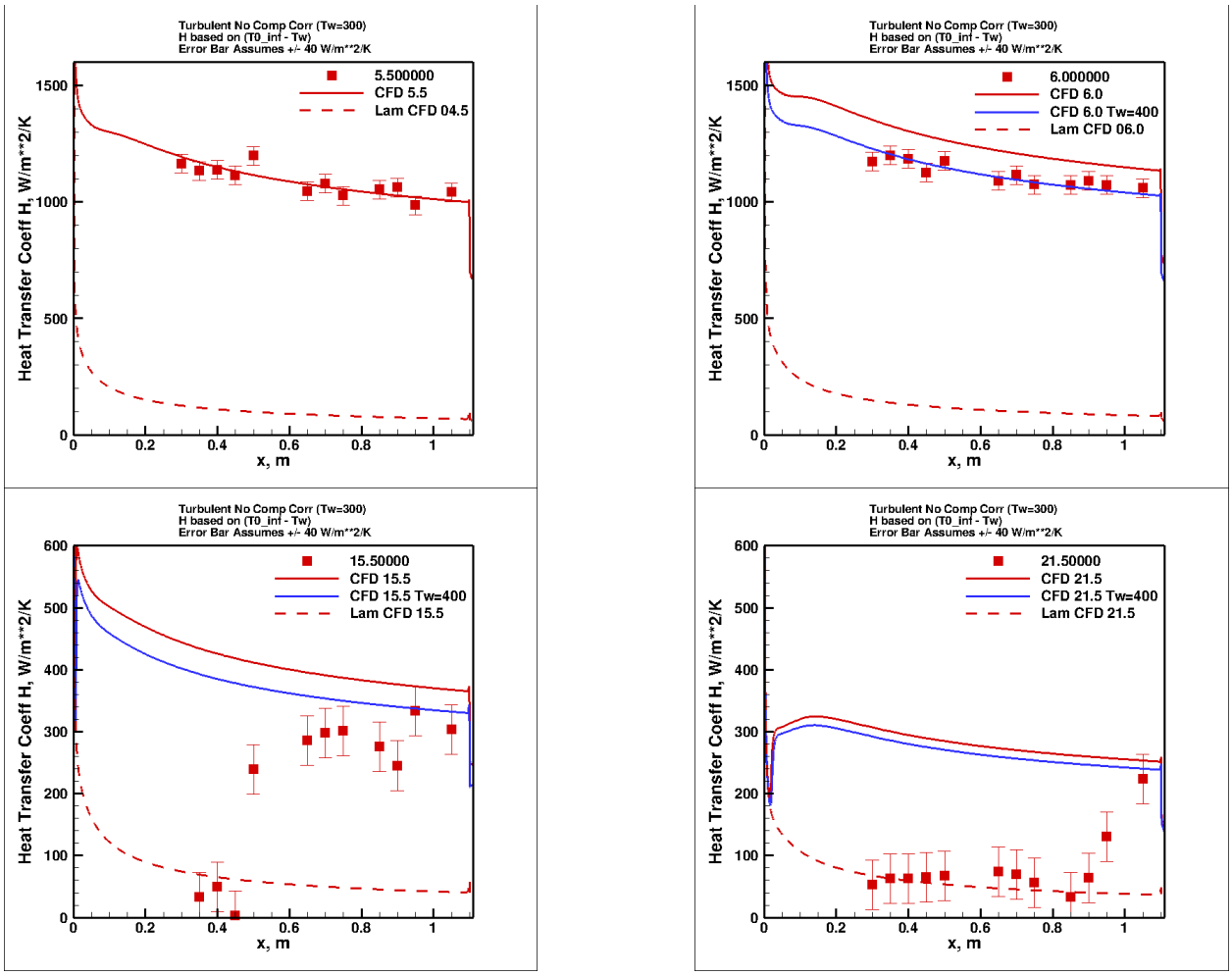

Figure 5 Measured and computed cone heat transfer at various times.

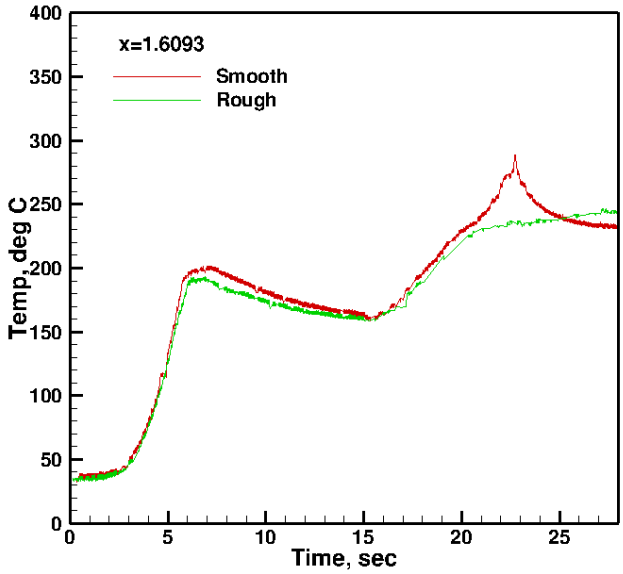

Figure 6 Measured smooth and rough-side temperatures on the flare during ascent.

V. Pressure

Figure 7 summarizes measured and computed pressure distributions in the SLBI at a variety of times during ascent. Rough-side data is included where available. Rough-side data agree with smooth-side data, within experimental scatter. Generally, the computation captures the upstream influence well. With the exception of t=5.5 seconds, computations agreed with measured pressures on the cylinder and flare until the second-stage burn began at t=16 seconds. After this time, measured and computed pressures on the cylinder agree will, but measured pressures on the flare deviate from the computations. The amount of deviation increases with time.

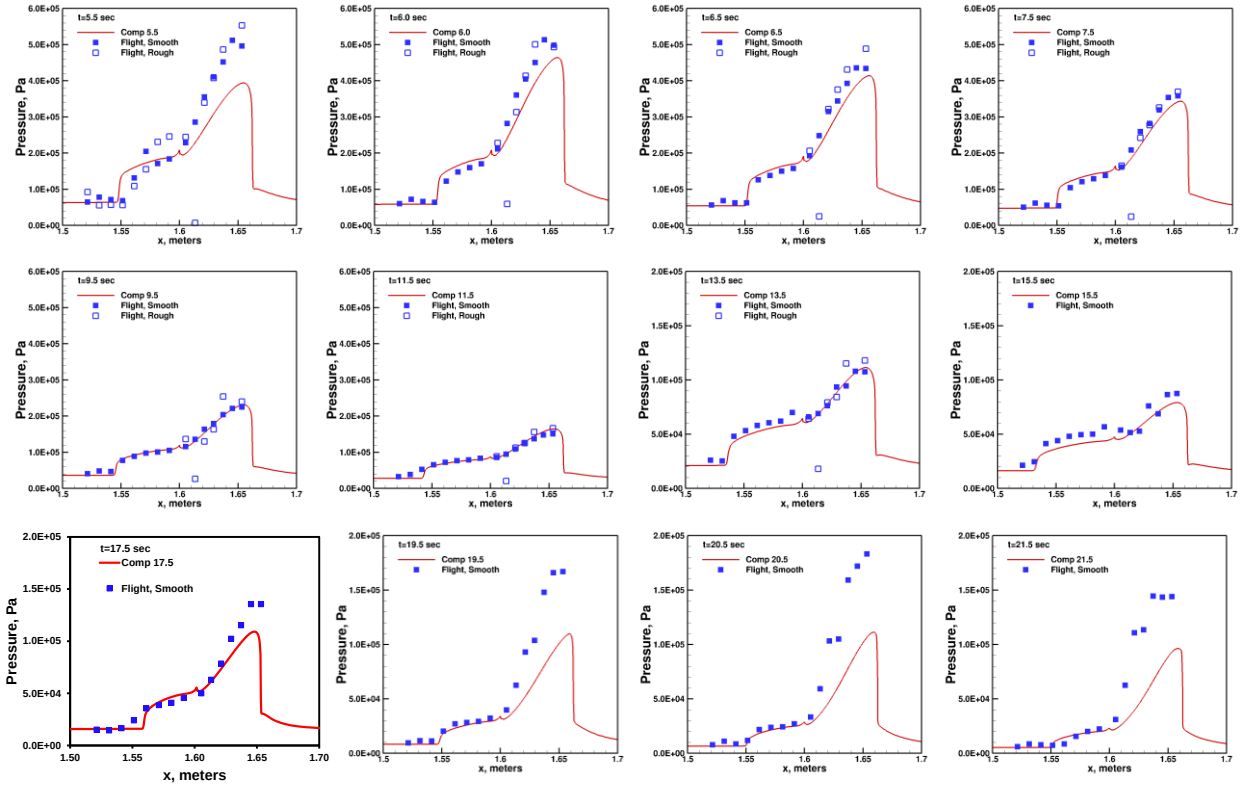

Figure 7 Measured and computed SBLI pressure distributions during ascent.

The temperature boundary condition was explored as a possible cause of the large pressure overshoots observed during second-stage burn. Figure 8 shows the effect of increasing the surface temperature from 300 K to 500 K. As expected, this has little effect on the surface pressures. Increased temperature causes a slight reduction in the computed surface pressure. The increased temperature causes a slight expansion of the upstream influence, probably due to the increase in boundary layer thickness attendant with the higher wall temperature.

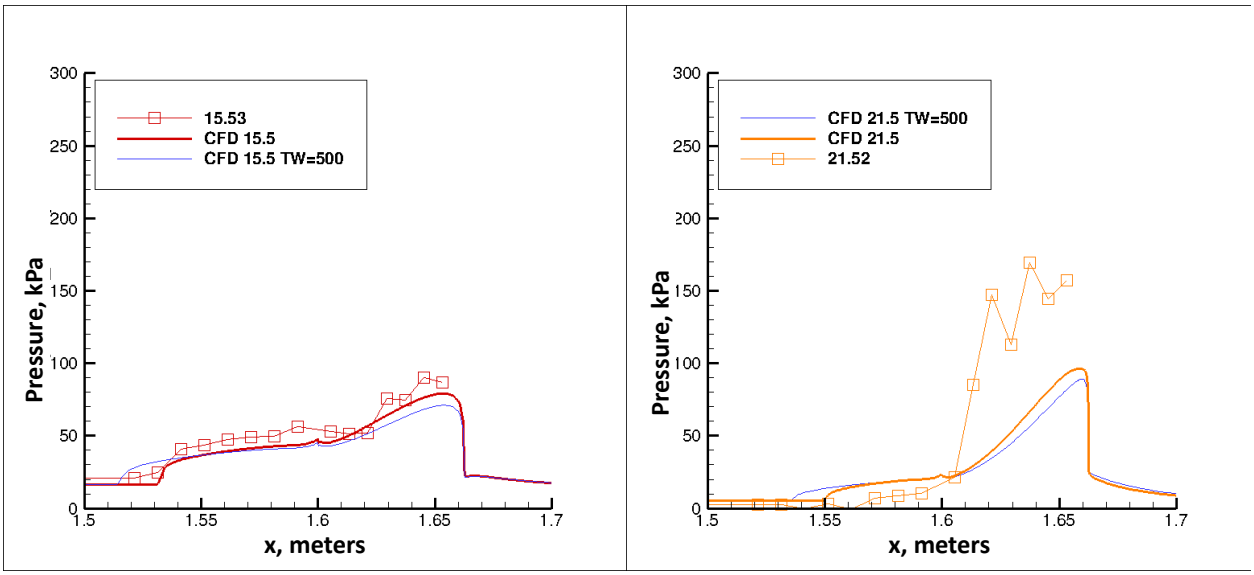

Figure 8 Effect of surface temperature on SBLI pressure

In order to understand the high pressures seen on the flare, the measured and computed pressures were compared to expected inviscid flare pressures. The inviscid flare pressures were derived from the Taylor-Maccoll solution for a 33° half-angle cone. For the times examined, the computations show undershoots of the inviscid pressure. For $t \leq 17.5$ seconds, the experimental data show either an undershoot or a modest overshoot. At later times, the measured pressures overshoot the inviscid levels by large amounts. Although some pressure overshoot is expected at reattachment in a SBLI, the measured flight pressures far exceed any overshoot amounts observed in ground test. For this reason, measured pressures on the flare for times greater than 17.5 seconds must be viewed with skepticism. Although some transitional effects may come into play for $t \geq 20$ seconds, the mechanism behind these large overshoots (either physical or due to measurement error) remains unknown.

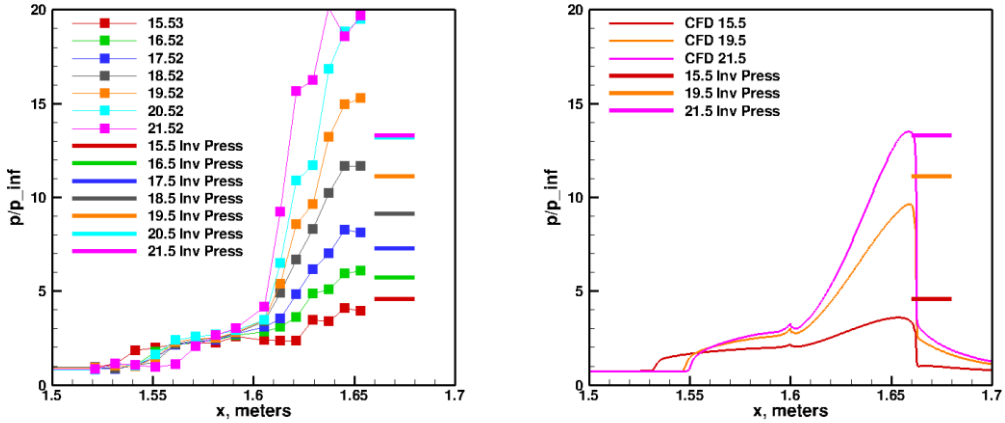

Figure 9 Measured and computed pressures compared to expected inviscid flare pressures.

VI. Heat Transfer

Figure 10 illustrates the comparison between measured and computed heat transfer in the SBLI after first-stage burnout. Since the CFD was computed at a constant wall temperature, and the experimental wall temperatures varied in space and time, the heating is compared on the basis of the convective heat transfer coefficient, *h*. The convective heat transfer coefficient h is evaluated based on the measured or computed temperature and the

stagnation temperature, $h = \dot{q}/(T_0 - T_w)$. Although the heat transfer coefficient is better evaluated using the recovery temperature, this quantity is difficult to evaluate, and the impact on heat transfer coefficient is minimal unless the wall temperature approaches the recovery temperature.

The agreement between the measured and computed heat transfer is fair, and this is due mostly to the large scatter in the measured heat transfer. This is especially true for t=15 and 17.5 seconds, when the heating rates were very low.

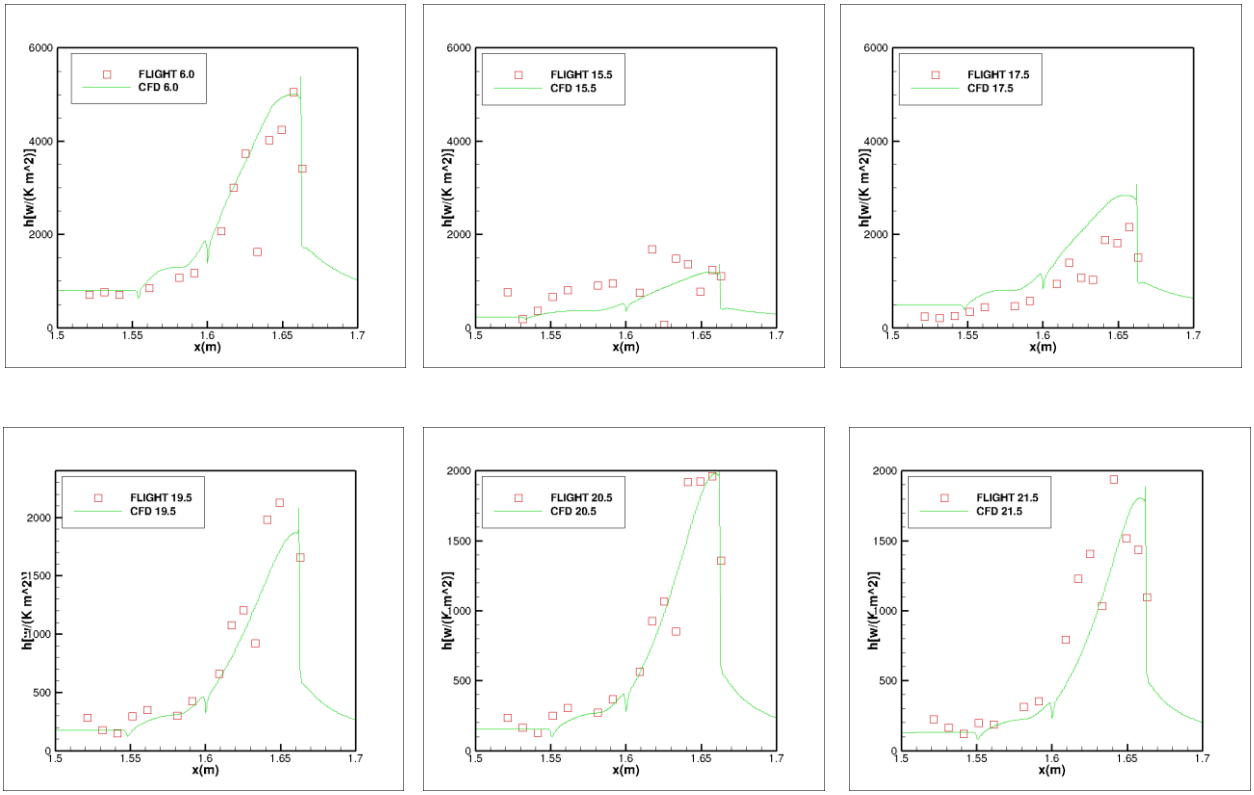

Figure 10 Measured and computed heat transfer.

VII. Conclusions and Future Work

The DPLR code using the SST turbulence model with no compressibility correction performed well in predicting the SBLI pressure and heat transfer over most of the HIFiRE-1 ascent. This performance is in agreement with expectations based on experimental / computational comparisons with ground tests at CUBRC at Mach 7. Flight data during the second-stage boost showed significant pressure overshoots on the flare. The mechanism behind these overshoots, or whether they are even physical or due to sensor malfunction, is unknown. Overall, the good agreement between the measured flight data and the computations helps to validate the strategy of calibrating CFD against wind tunnel tests prior to exercising codes at flight conditions.

The final version of this paper will include additional details of the computational methods and additional analysis of the SBLI.

Acknowledgments

This work was supported by the United States Air Force Research Laboratory and the Australian Defence Science and Technology Organisation and was carried out under Project Agreement AF-06-0046. Many thanks are extended to RANRAU, AOSG, WSMR/DTI/Kratos and all members of the DSTO AVD Team Brisbane. The authors also wish to acknowledge the efforts and support of Douglas Dolvin and John Schmisseur, AFRL. The BEA was provided by Mary Bedrick of Detachment 3 Air Force Weather Agency. Scott Stanfield of Spectral Energies / ISSI assisted in data analysis. Mark Smith of NASA DFRC developed the BET

References

[1] Dolvin, D. "Hypersonic International Flight Research and Experimentation (HIFiRE) Fundamental Science and Technology Development Strategy," AIAA Paper 2008-2581, April 2008.

[2] Dolvin, D. J., "Hypersonic International Flight Research and Experimentation Technology Development and Flight Certification Strategy," AIAA paper 2009-7228, October 2009.

[3] Kimmel, R. L., Adamczak, D., Gaitonde, D., Rougeux, A., Hayes, J. R., "HIFiRE-1 Transition Experiment Design," AIAA paper 2007-0534, January 2007.

[4] Wadhams, T. P., MacLean, M. G., Holden, M.S., and Mundy, E., "Pre-Flight Ground Testing of the Full-Scale FRESH FX-1 at Fully Duplicated Flight Conditions," AIAA paper 2007-4488, June 2007.

[5] Johnson, H. B., Alba, C. R., Candler, G. V., MacLean, M., Wadhams, T, and Holden, M. "Boundary Layer Stability Analysis of the Hypersonic International Flight Research Transition Experiments," *AIAA Journal of Spacecraft and Rockets*, Vol. 45, No. 2, March-April 2008, pp 228-236.

[6] Holden, M. S., Wadhams, T. P., MacLean, M., "Experimental Studies in the LENS Supersonic and Hypersonic Tunnels for Hypervelocity Vehicle Performance and Code Validation," AIAA paper 2008-2505, April 2008.

[7] Kimmel, R. L., "Aerothermal Design for the HIFiRE-1 Flight Vehicle," AIAA paper 2008-4034, June 2008.

[8] Casper, K. M., Johnson, H. B., and Schneider, S. P., "Effect of Freestream Noise on Roughness-Induced Transition for a Slender Cone," *AIAA Journal of Spacecraft and Rockets*, vol. 48, no. 3, May-June 2011, pp 406-413.

[9] Kimmel, R. L., "Roughness Considerations for the HIFiRE-1 Vehicle," AIAA Paper 2008-4293, June 2008.

[10] Alba, C. R., Johnson, H. B., Bartkowicz, M. D., Candler, G. V., and Berger, K. T. "Boundary-Layer Stability Calculations for the HIFiRE-1 Transition Experiment," *AIAA Journal of Spacecraft and Rockets*, Vol. 45, No. 6, November-December 2008, pp. 1125-1133.

[11] Wadhams, T. P., Mundy, E., MacLean, M. G., and Holden, M. S., "Ground Test Studies of the HIFiRE-1 Transition Experiment Part1: Experimental Results," *AIAA Journal of Spacecraft and Rockets*, Vol. 45, No. 6, November-December 2008, pp. 1134-1148.

[12] MacLean, M., Wadhams, T., Holden, M., and Johnson, H., "Ground Test Studies of the HIFiRE-1 Transition Experiment Part 2: Computational Analysis," *AIAA Journal of Spacecraft and Rockets*, Vol. 45, No. 6, November-December 2008, pp. 1149-1164.

[13] Berger, K. T., Greene, F. A., Kimmel, R. L., Alba, C., and Johnson, H., "Erratum on Aerothermodynamic Testing and Boundary-Layer Trip Sizing of the HIFiRE Flight 1 Vehicle," *AIAA Journal of Spacecraft and Rockets*, Vol. 46, No., 2, March-April, 2009, pp. 473-480.

[14] Adamczak, D., Alesi, H., Frost, M., "HIFiRE-1: Payload Design, Manufacture, Ground Test, and Lessons Learned," AIAA paper 2009-7294, October 2009.

[15] Kimmel, R. L., Adamczak, D., and Brisbane DSTO-AVD Team, "HIFiRE-1 Preliminary Aerothermodynamic Measurements," AIAA paper 2011-3413, June 2011.

[16] Stanfield, S. A., Kimmel, R. L., and Adamczak, D., "HIFiRE-1 Data Analysis: Boundary Layer Transition Experiment During Reentry," AIAA paper 2012-1087, January 2012.

[17] Kimmel, R., L., Adamczak, D., Stanfield, S., Borg, M., "Analysis of HIFiRE-1 Transition Data," NATO Research and Technology Agency, Specialists Meeting AVT-200/RSM-030 on Hypersonic Laminar-Turbulent Transition, paper MP-AVT-200-02, San Diego, CA, 14-17 May 2012.

[18] Stanfield, S., Kimmel, R. L., and Adamczak, D., "HIFiRE-1 Flight Data Analysis: Turbulent Shock-Boundary-Layer Interaction Experiment During Ascent," AIAA paper 2012-2703, June 2012.

[19] Smart, M. K., Hass, N. E., and Paull, A., "Flight Data Analysis of the HyShot 2 Scramjet Flight Experiment," AIAA Journal, Vol. 44, No. 10, October 2006, pp. 2366-2375.

[20] Walker, S., and Rodgers, F., "The Hypersonic Collaborative Australia/United States Experiment (HyCAUSE)," AIAA paper 2005-3254, May 2005.

[21] Adamczak, D., Kimmel, and Brisbane DSTO-AVD Team, "HIFiRE-1 Flight Trajectory Estimation and Initial Experimental Results," AIAA paper 2011-2358, May 2011.